

Supporting information

Fe-V@NiO heterostructure electrocatalyst towards oxygen evolution reaction

Yu-Xun Zhu^a, Mei-Yan Jiang^a, Min Liu^c, Lian-Kui Wu^{a, b, *}, Guang-Ya Hou^a, Yi-Ping Tang^a

a. College of Materials Science and Engineering, Zhejiang University of Technology,

Hangzhou 310014, China

b. School of Materials, Sun Yat-sen University, Guangzhou 510275, China

c. State Grid Zhejiang Electric Power Research Institute, Hangzhou 310014, China

E-mail: wulk5@mail.sysu.edu.cn

Experimental

Chemicals and Regions

Nickel (II) nitrate hexahydrate ($\text{Ni}(\text{NO}_3)_2 \cdot 6\text{H}_2\text{O}$, > 99%), ammonium fluoride (NH_4F , > 99%), iron (III) chloride hexahydrate ($\text{FeCl}_3 \cdot 6\text{H}_2\text{O}$, > 99%), vanadium (III) chloride (VCl_3 , > 97%), and urea (H_2NCONH_2 , > 99%) were purchased from Shanghai Macklin Biochemical Technology Co. Ltd.. Hydrochloric acid (HCl , > 99%), potassium hydroxide (KOH , > 99%), and ethanol ($\text{CH}_3\text{CH}_2\text{OH}$, > 99%) were obtained from Hangzhou Xiao Shan chemical reagent factory. All chemical reagents were used as received without further purification. Deionized (DI) water was used in all experiments.

Ni foam (NF, thickness: 1.5 mm, bulk density: 0.28 g cm^{-3} ; number of pores per inch: 110) was purchased from Kunshan JiaYiSheng electronics. Co. Ltd.. Before

hydrothermal, NF was immersed into 4.0 mol L⁻¹ HCl for 5 min, then washed with a plenty of running water and rinsed with DI water in an ultrasonic bath for 5 min, finally washed with ethanol for several times and blow-dried.

Fabrication of NiO/NF

6.0 mmol of Ni(NO₃)₂·6H₂O, 12.0 mmol of NH₄F and 15 mmol of urea were dissolved in 60 ml of DI water to form a clear solution, which was transferred into a 100 mL Teflon-lined autoclave with a piece of Ni foam (size: 1.0 × 3.0 cm²). The autoclave was sealed and maintained at 100 °C for 12 h. Then the obtained Ni(OH)₂/NF was taken out from the autoclave and washed by a plenty of DI water. Finally, Ni(OH)₂/NF was further calcined at 450 °C for 2 h in air with a heating rate of 5 °C min⁻¹ to form NiO/NF electrode.

Fabrication of Fe-V@NiO/NF

0.8 mmol of FeCl₃·6H₂O, 0.8 mmol of VCl₃ and 2.5 mmol of urea were dissolved in 40 ml of DI water to form a clear solution, which was transferred into a 100 mL Teflon-lined autoclave with the previously obtained NiO/NF electrode. The autoclave was sealed and maintained at 120 °C for 12 h. Then, the electrode was taken out from the autoclave and washed with a plenty of DI water and dried by warm air. Finally, Fe-V@NiO/NF electrode was formed.

Fabrication of Fe-V/NF

For comparison, Fe-V/NF was also fabricated by using NF instead of NiO/NF during the preparation of Fe-V@NiO/NF.

Electrochemical oxidation

To optimized the OER performance, all specimens were acted as anodes and treated by a galvanostatic treatment in 1.0 M KOH at current density of 10 mA cm⁻². Specimen denoted as Fe-V@NiO/NF₁₀, Fe-V/NF₁₀ and NiO/NF₁₀ indicate that the in situ oxidation process was lasted for 10 h.

Physical-chemical Characterization

Grazing Incidence XRD (XRD) with a grazing incidence angle of 0.8° of the specimens were recorded on a RIGAKU D/Max 2550 PC diffractometer equipped with Cu K α radiation ($\lambda=1.54059$ Å) at 40 kV and 30 mA. Raman spectra of the materials were collected from 200 to 1400 cm⁻¹ on a Renishaw 2000 Confocal Raman Microprobe (Renishaw Instruments, England) using a 20 mW air- cooled argon ion laser (523 nm). The morphology and composition of the specimens were characterized by field emission scanning electron microscopy (FE-SEM, Carl Zeiss Supra 55) equipped with energy dispersive X-ray (EDX) microanalysis (Oxford EDS Inca Energy Coater 300) and atomic force microscopy (AFM, Bruker Dismension Icon 3 atomic force microscope). Transmission electron microscopy (TEM) and high-resolution TEM (HR-TEM) images were acquired on a Tecnai G2 F30 (Philips-FEI, Co. Ltd) instrument at an acceleration voltage of 300 kV. The surface chemical state and composition of the materials were investigated by X-ray Photoelectron Spectroscopy (XPS, Kratos AXIS Ultra DLD using monochromatized Al K α excitation).

Electrochemical measurements

Linear sweep voltammetry (LSV) and cyclic voltammetry (CV) measurements were carried out on CS 310H. All electrochemical tests were operated at 25 \pm 1 °C in 1.0 M

KOH solution. A three-electrode system was employed for measurement, where the Fe-V@NiO/NF was directly used as the working electrode, an Ag/AgCl electrode and a platinum plate with an exposed area of 4.0 cm² were used as reference and counter electrodes, respectively. Potentials vs. RHE are calculated using the Nernst equation $E_{\text{RHE}} = E_{\text{Ag/AgCl}} + 0.0591(\text{pH}) + 0.1976$. LSV measurements were carried out between 0.2 and 1.2 V vs. Ag/AgCl with scan rate of 1.0 mV s⁻¹. The polarization curves were IR-corrected as following: $E = E_{\text{apply}} - iR$ (i is current at a particular potential and R is solution resistance tested by electrochemical impedance spectroscopy measurement.). CV tests were conducted to evaluate the electrochemical double layer capacitance at non-faradaic potential region. In detail, a series of CV measurements were performed within the potential window from 0 to 0.1 V vs. Ag/AgCl at various scan rates from 20 to 100 mV s⁻¹. Electrochemical impedance spectroscopy (EIS) measurements were carried out at 0.55 V vs. Ag/AgCl over the frequency range from 100 kHz to 10 mHz with the AC amplitude of 5 mV. Chronoamperometric measurements were tested on corresponding potential to support a current density of about 10 mA cm⁻² for 10 h.

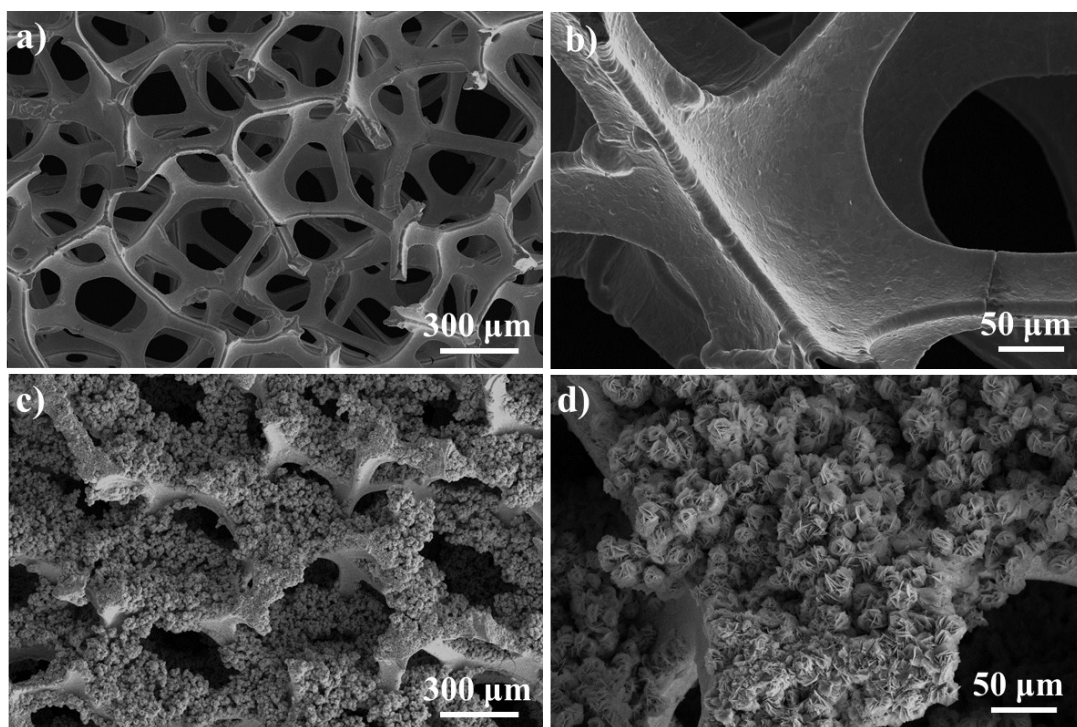


Fig. S1 SEM images of bare NF (a, b), and NiO/NF₀ (c, d).

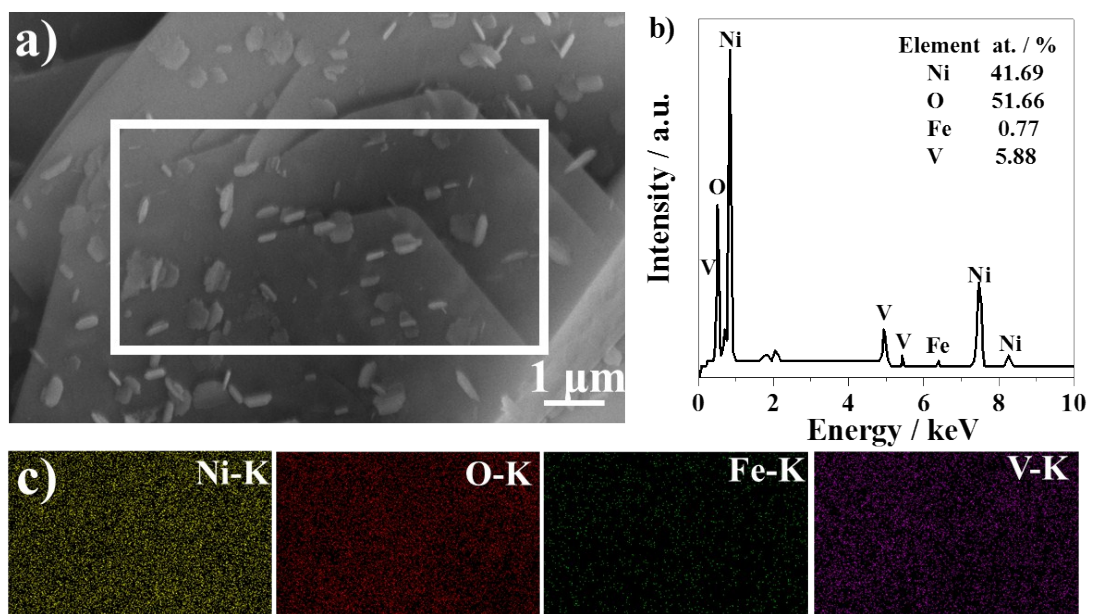


Fig. S2 SEM images, EDX patterns, and corresponding elemental mapping images of Fe-V@NiO/NF₀.

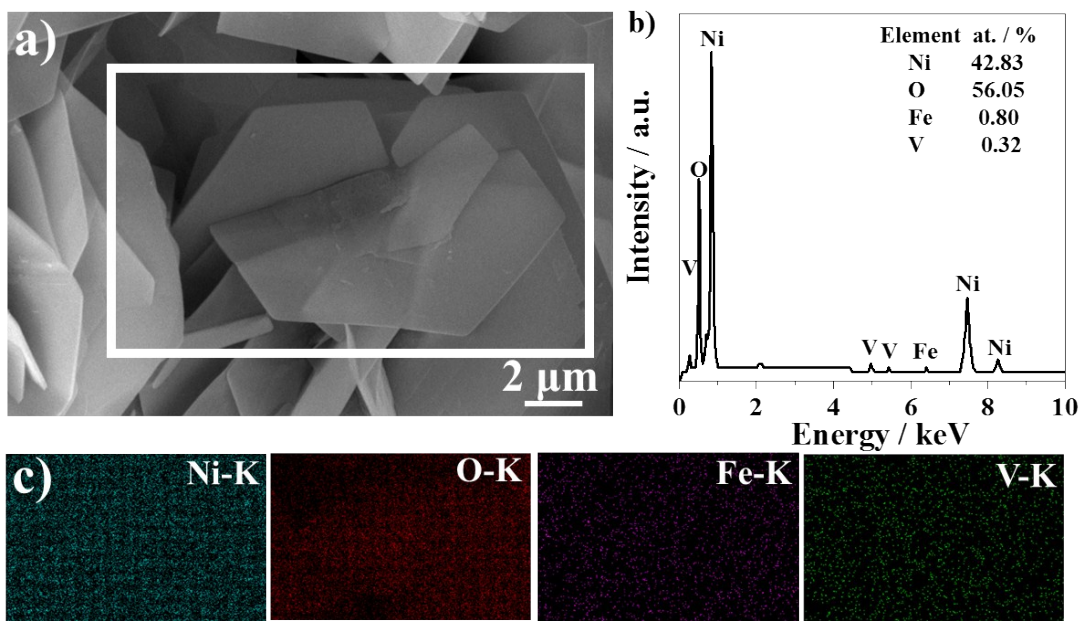


Fig. S3 SEM images, EDX patterns, and corresponding elemental mapping images of Fe-V@NiO/NF₁₀.

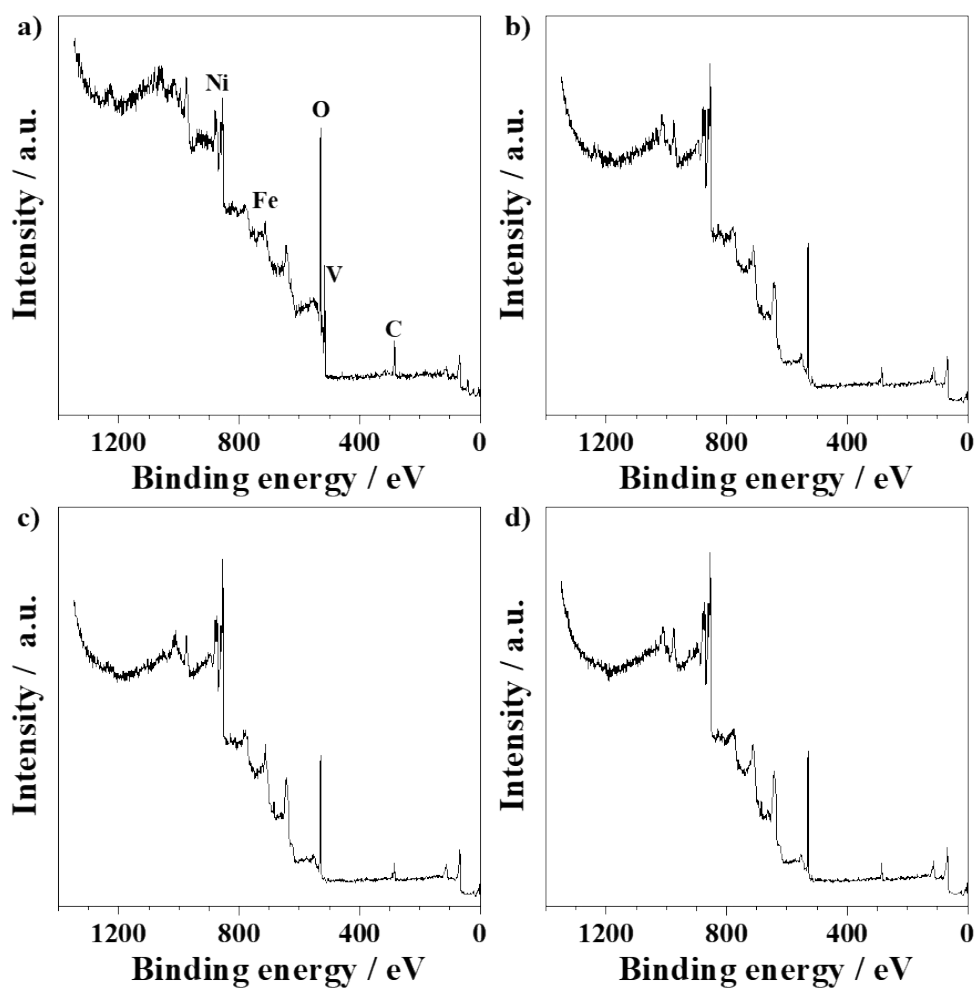


Fig. S4 XPS Survey spectra of Fe-V@NiO/NF₀ (a), Fe-V@NiO/NF₂ (b), Fe-V@NiO/NF₆ (c), Fe-V@NiO/NF₁₀ (d).

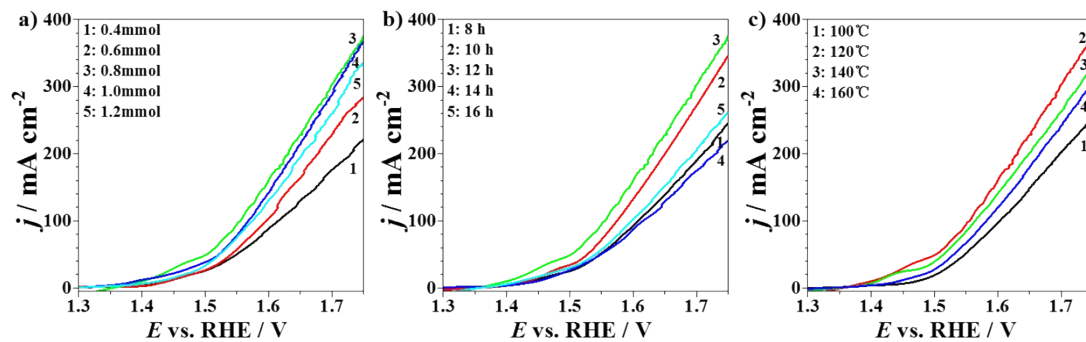


Fig. S5 The influence of Fe^{3+} and V^{3+} concentrations (a), hydrothermal time (b), and hydrothermal temperature (c) on the LSV performance of Fe-V@NiO/NF_{10} .

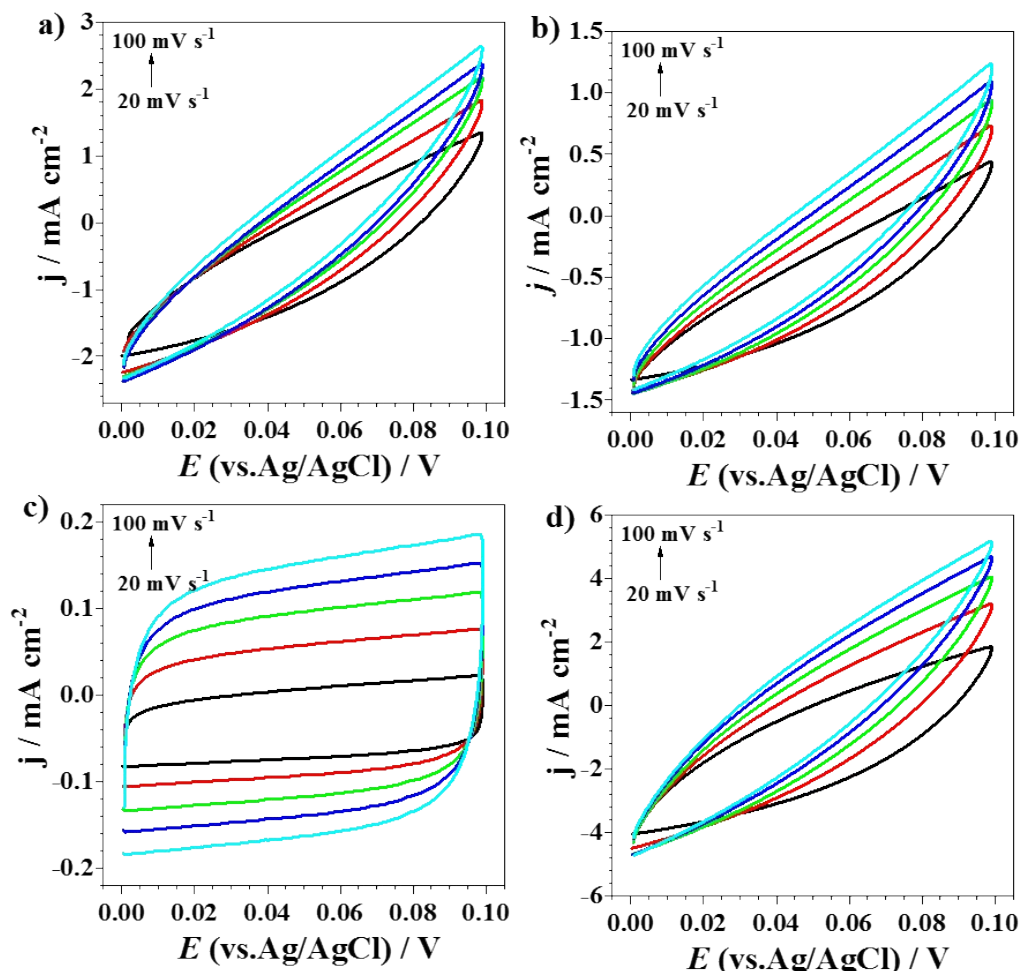


Fig. S6 CV curves in the double layer region with various scan rates from 20 to 100 mV s^{-1} for different electrodes: Fe-V@NiO/NF₁₀ (a), Fe-V@NiO/NF₀ (b), Fe-V/NF₁₀ (c), and NiO/NF₁₀ (d).

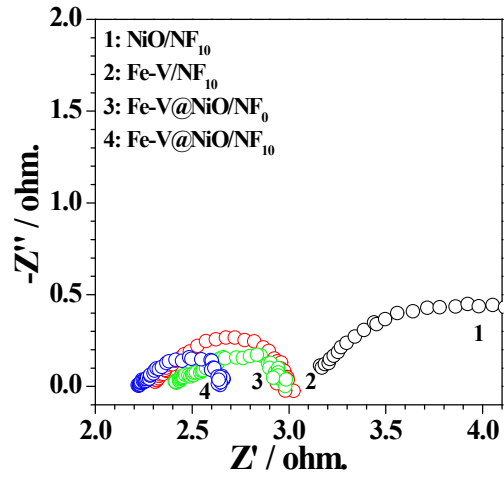


Fig. S7 Nyquist plots of the NiO/NF₁₀ (1), Fe-V/NF₁₀ (2), Fe-V@NiO/NF₀ (3), Fe-V@NiO/NF₁₀ (4).

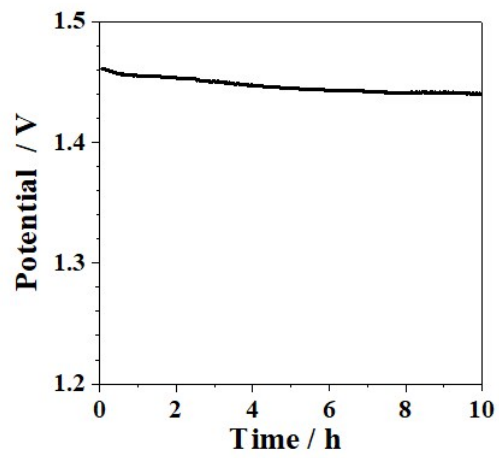


Fig. S8 The evolution of electrode potential for Fe-V@NiO/NF₀ when electrolysis at current density of 10 mA cm⁻² in 1.0 M KOH.

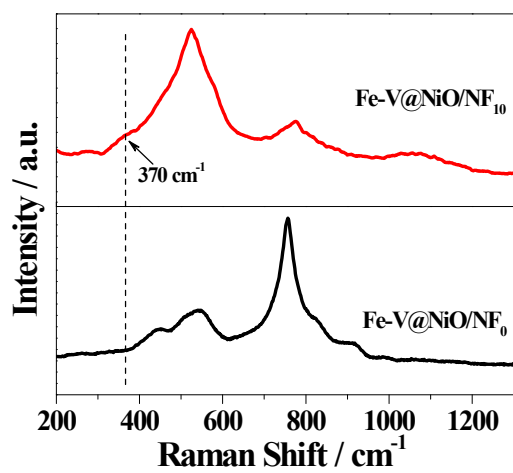


Fig. S9 Raman spectra of Fe-V@NiO/NF₀ and Fe-V@NiO/NF₁₀.

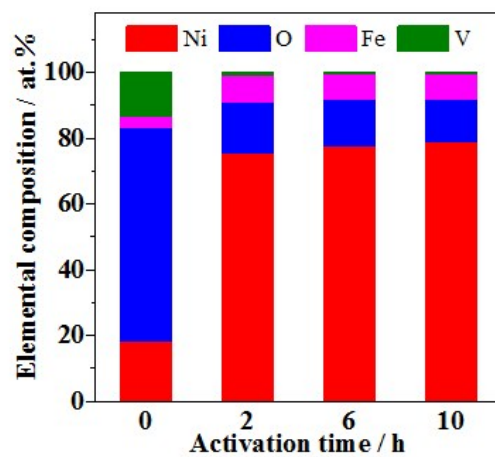


Fig. S10 Elemental composition of Fe-V@NiO/NF after oxidation treatment for different periods.

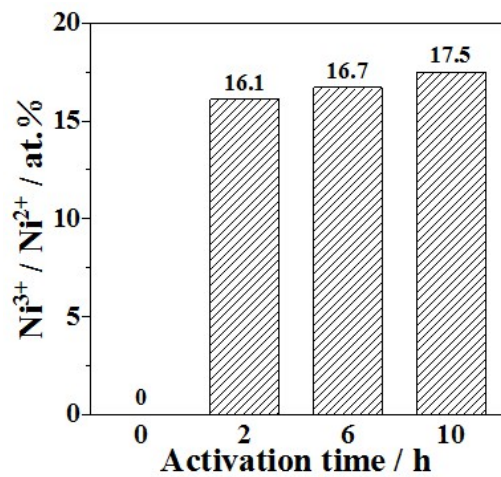


Fig. S11 The valence state ratio of nickel ($\text{Ni}^{3+} / \text{Ni}^{2+}$) of Fe-V@NiO/NF after oxidation treatment for different periods.

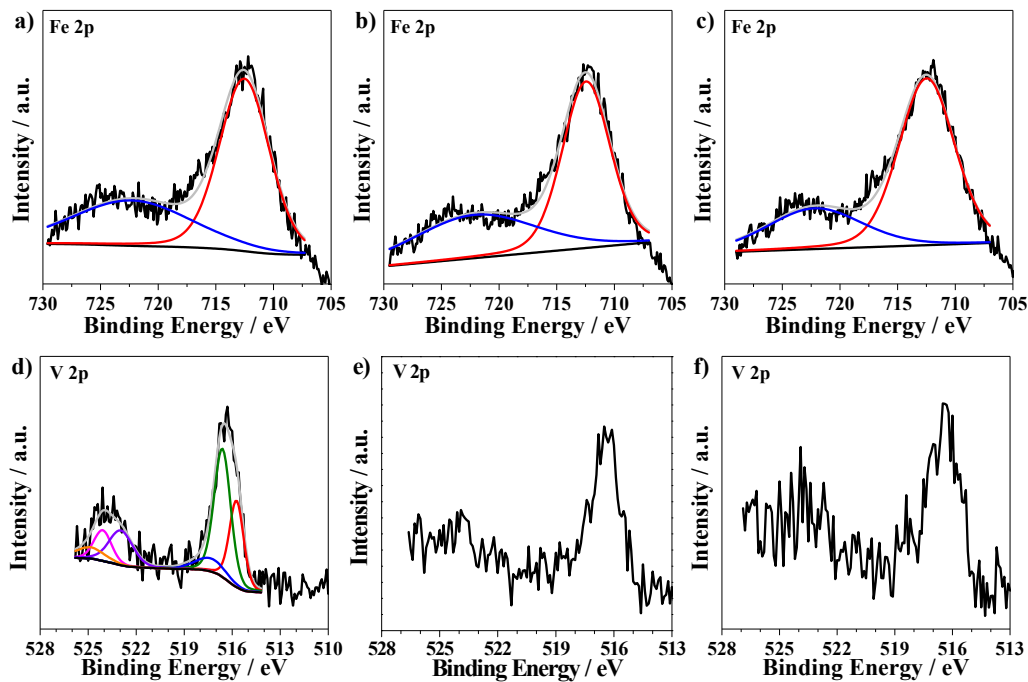


Fig. S12 High-resolution XPS spectra of Fe 2p (a-c) and V 2p (d-f) of Fe-V@NiO/NF₂ (a, d), Fe-V@NiO/NF₆ (b, e), and Fe-V@NiO/NF₁₀ (c, f).